Electronic Supplementary Material (ESI) for Journal of Materials Chemistry A.

Supporting Information

The comprehensive utilization of the synergistic effect of fullerene and non-fullerene acceptors to achieve highly efficient polymer solar cells

Zezhou Liang,[a] Junfeng Tong,[a] Hongdong Li,[c] Yufei Wang,[a] Ningning Wang,[a] Jianfeng Li*,[a] Chunming Yang,*,[b] and Yangjun Xia[a]

[a] School of Materials Science and Engineering, Lanzhou Jiaotong University, Lanzhou, 730070, P. R. China. E-mail: ljfpyc@163.com

[b] Shanghai Synchrotron Radiation Facility, Shanghai Advanced Research Institute, Chinese Academy of Sciences, 239 Zhang Heng Road, Pudong New District, Shanghai 201204, China. E-mail: yangchunming@zjlab.org.cn

[c] CAS Key Laboratory of Nanosystem and Hierarchical Fabrication, CAS Center for Excellence in Nanoscience, National Center for Nanoscience and Technology, Beijing, 100190, China.

Experimental Section

Materials

$PC_{71}BM$ (99.5%) was purchased from Sigma Aldrich and IT-M was purchased from Solarmer Materials Inc.

Device fabrication and characterization

Indium tin oxide (ITO) coated glass substrates were washed by a wet-cleaning process inside an ultrasonic bath, with de-ionized water, acetone, de-ionized water and isopropanol in turn. After drying under nitrogen flow, the substrates were treated with oxygen plasma for 6 min, then a thin layer of poly(3,4-ethylenedioxythiophene):poly(styrene-sulfonate) (PEDOT:PSS, ca. 40 nm, Clevios PVP Al4083) was spin-coated onto the ITO substrates and annealed at 160 C^{o} for 20 min. After that the substrates were transferred into a nitrogen-filled glove box and the active layer was prepared. PTBTz-2: IT-M (total concentration 25mg mL^{-1}, 1:1.5) solutions were prepared from a blended solution of chlorobenzene (CB) with 0.5vol% of 1,8-diiodooctane (DIO), and the introduced $PC_{71}BM$ proportionated to a acceptor component weight ratio of IT-M:$PC_{71}BM$ were 10%, 20%, 30%, 40%, 50% , 60%, 70%, 80% and 90%, respectively. And binary devices PTBTz-2: $PC_{71}BM$ (1:1.5, total concentration 25mg mL^{-1}, 1:1.5, 3vol% DIO) were fabricated as substance device. Then, an ultrathin layer of PDINO (1mg mL^{-1} in methanol) was spin-coated on the active layer. Finally, the aluminium layer (~100 nm) as the cathode was thermally evaporated under a vacuum pressure of 10^{-4} Pa. The conventional PSCs's structure is ITO/PEDOT:PSS/PTBTz-2: IT-M :$PC_{71}BM$ /PDINO/Al. Under each condition, at least 15 separated devices were fabricated to calculate the average PCEs. Moreover, the all effective device area in this work was 0.1 cm^2, which was ascertained by a shadow mask. The current density-voltage (*J-V*) characteristics were measured in the dark and under simulated 100 mW/cm^2 (AM 1.5G) irradiation from a Newport solar simulator using a Keithley 2400 source meter instrument unit. External quantum efficiencies (EQEs) were measured using an incident photon-to-charge carrier efficiency (IPCE) setup (7-SCSpecIII, Beijing 7-star Optical Instruments Co.) equipped with a standard Si diode. The ultraviolet-visible (UV-visible) absorption spectra were recorded on a UV-1800 spectrophotometer (Shimadzu, Kyoto, Japan). The morphologies of the films were characterized by a tapping-mode atomic force microscope (AFM, Agilent 5400) and transmission electron microscope (HITACHI

H-7650). Grazing incidence wide-angle X-ray scattering (GIWAXS) patterns were acquired by beamline BL16B1 (Shanghai Synchrotron Radiation Facility)[1]. The X-ray wavelength was 0.124 nm (E=10 keV), and the incidence angle was set to 0.2 degree.

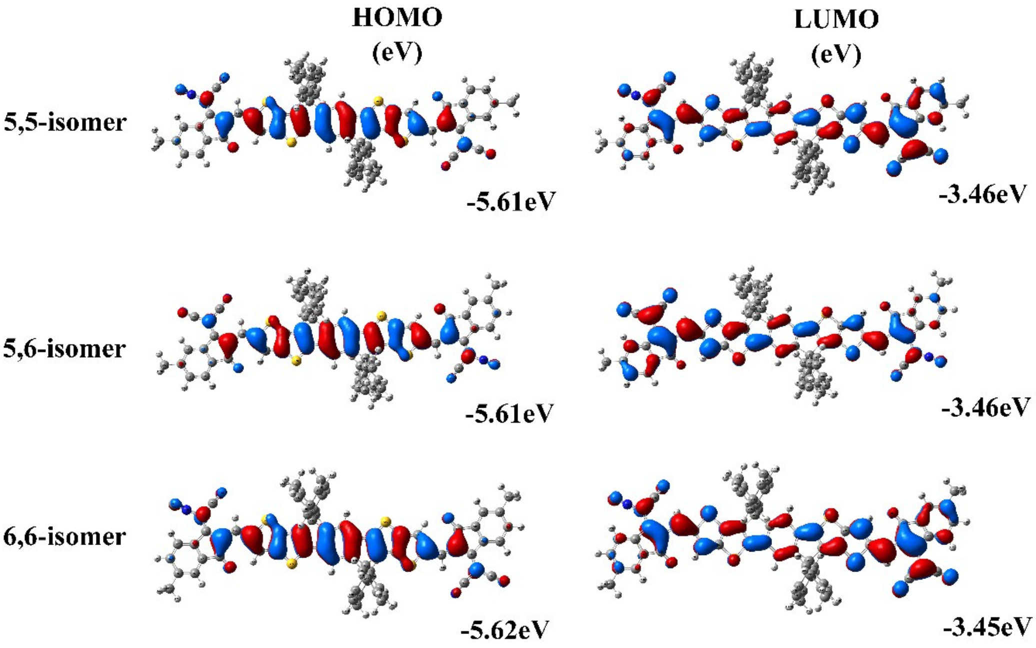

Figure S1. Theoretical calculation results of the three isomers in IT-M.

Calculation of DOS of collaborative unit

Here, N_e of $PC_{71}BM$ and the three isomers of IT-M can be calculated by $N_e = nl$, where n is the molecular number of unit mass, and l is the number of quasi-degenerate LUMOs (<0.1 eV) of per molecular. Here, N_{e1} of $PC_{71}BM$ is $2 \times 6.02 \times 10^{23}/1030\ g^{-1} = 1.17 \times 10^{21}\ g^{-1}$. And N_{e2} of IT-M is $1 \times 6.02 \times 10^{23}/1456 = 4.13 \times 10^{20} g^{-1}$.

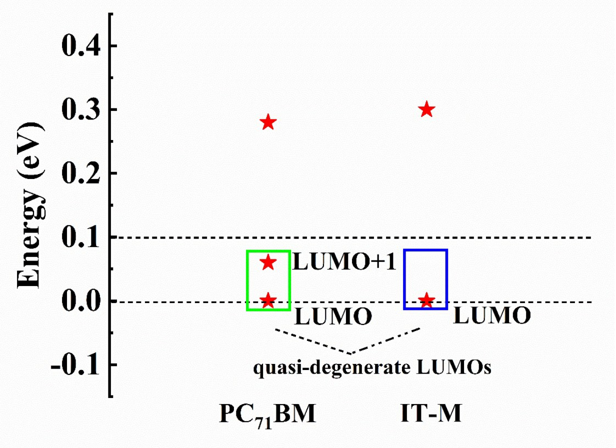

Figure S2 Diagram of the frontier orbital energies of neutral PC71BM and IT-M. The date of $PC_{71}BM$ is reported by T. Liu et al[2].

Table S1 Calculated $G_{\max}$ with different $PC_{71}BM$ content.

$PC_{71}BM$ (wt %)	J_{SC}/J_{sat}	G_{max} (m^{-3} s^{-1}) (J_{sat})
0%	95.68%	1.278×10^{28} (18.41)
10%	94.22%	1.351×10^{28} (19.46)
20%	96.06%	1.352×10^{28} (19.47)
30%	95.93%	1.322×10^{28} (19.04)
40%	93.77%	1.313×10^{28} (18.91)
50%	95.11%	1.273×10^{28} (18.33)
60%	94.58%	1.268×10^{28} (18.26)
70%	94.13%	1.263×10^{28} (18.19)
80%	93.63%	1.258×10^{28} (18.12)
90%	94.17%	1.241×10^{28} (17.87)
100%	94.63%	1.201×10^{28} (17.30)

$G_{max}= J_{sat}/qL$, L is the thickness of active layers, L=90nm.

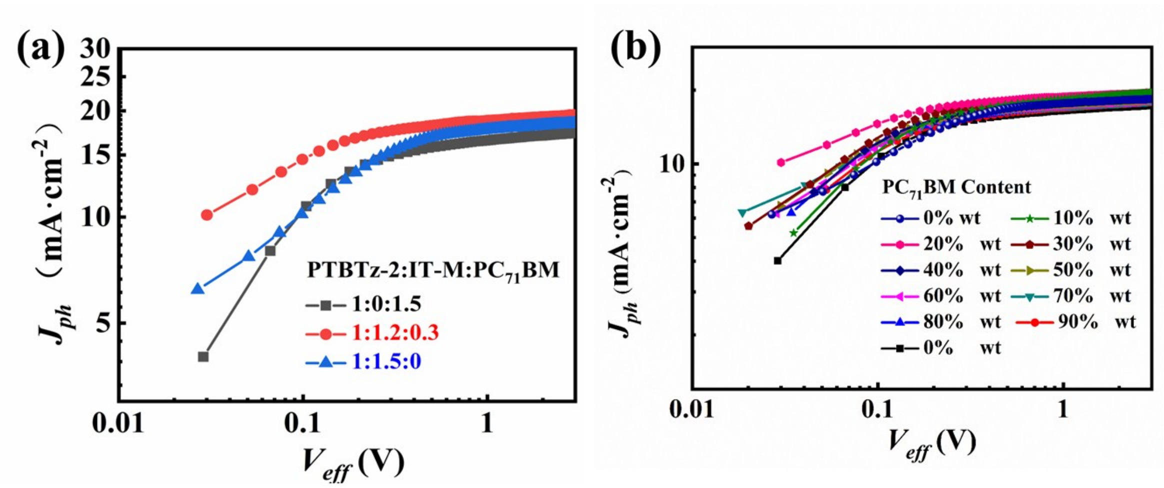

Figure S3. The J_{ph}–V_{eff} curves for all the ternary solar cells with different $PC_{71}BM$ weight ratio.

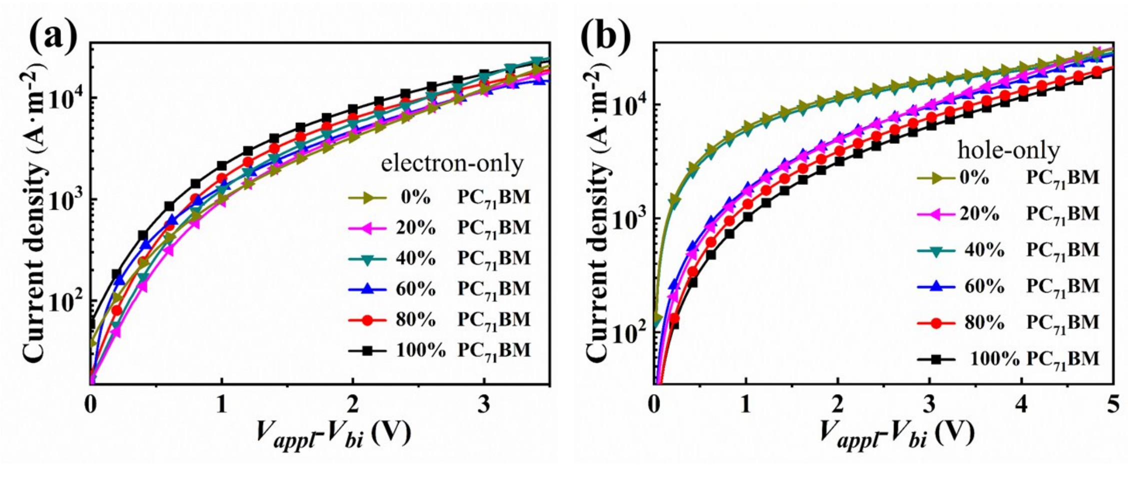

Figure S4. The *J–V* curves of: (a) electron-only and (b) hole-only devices with different $PC_{71}BM$ doping ratios.

Surface energy analysis

Table S2 Surface energies of PTBTz-2, IT-M and $PC_{71}BM$ film.

materials	Contact angle (°)		Surface energy γ (mNm^{-1})
	deioninzed water	diiodomethane	
PTBTz-2	102.5	53.3	33.46
IT-M	96.9	35.6	43.22
$PC_{71}BM$	93.5	25.9	47.18

Table S3 Interfacial surface energy of different materials.

Material	**Interfacial surface energy (m*J*/cm^2)**
$\gamma_{PC71BM\text{-}IT\text{-}M}$	0.25
$\gamma_{PC71BM\text{-}PTBTz\text{-}2}$	2.88
$\gamma_{PTBTz\text{-}2\text{-}IT\text{-}M}$	1.45

The interfacial surface energy (γ_{X-Y}) between X and Y in the blend films can be calculated by the equation[3],

$$\gamma_{X-Y} = \gamma_X - \gamma_Y - 2\sqrt{\gamma_X \cdot \gamma_Y} \cdot e^{\left[-\beta(\gamma_X - \gamma_Y)^2\right]} \qquad (1)$$

Where $\beta = 0.000115\ m^4/mJ^2$.

The wetting coefficient (ω_C) of a material C ($PC_{71}BM$) in blends of host materials A

(PTBTz-2) and B (IT-M), which can predict the location of C in ternary blends, can be calculated using Young's equation[4],

$$\omega_C = \frac{\gamma_{C-B} - \gamma_{C-A}}{\gamma_{A-B}} \qquad (2)$$

If the wetting coefficient is larger than unity ($\omega_C > 1$), C will be located in domains of A. If $\omega_C < -1$, C will be located in domains of B. If $-1 < \omega_C < 1$, C will be located at the interface between domains of A and B.

Hole and electron mobility measurement

The hole-only mobility (μ_h) was characterized from the device with the configuration of ITO/PEDOT:PSS/active layer (110 nm)/MoO_3/Ag, while electron-only mobility (μ_e) was measured from the device with the configuration of ITO/ZnO/active layer (110 nm)/PDINO/Al. All the blend films were prepared in accordance with the optimal solar cells conditions. The obtained current−voltage curves were consistent with the Mott−Gurney square law, given by Equation (3)

$$J_{SCLC} = (\frac{9}{8})\varepsilon_0\varepsilon_r\frac{(V_{appl} - V_{bi})}{L^3} \qquad (3)$$

Where J is the current density, ε_0 is the permittivity of free space (≈8.85×10^{-14} Fcm^{-1}), ε_r is the relative dielectric constant of the organic active layer (≈3.00), L is the thickness of the active layer, V_{appl} is the applied voltage on the device, V_{bi} is built-in voltage, μ is the mobility. V_{bi} of electron-only device and hole-only device are 0.7 and 0 V, respectively.

Time-correlated single photon counting (TCSPC)

Time-correlated single photon counting (TCSPC) is a convenient tool to investigate the energy or charge transfer between different molecules. TCSPC detects single photons of a periodic light signal and determines the times of the photons after the excitation pulses. The pulse repetition rate of the signal is much higher than the photon detection rate. Therefore, the detection of several photons per signal period is extremely unlikely. Only a single photon per signal period needs to be considered. The time of this photon can be determined at extremely high resolution.

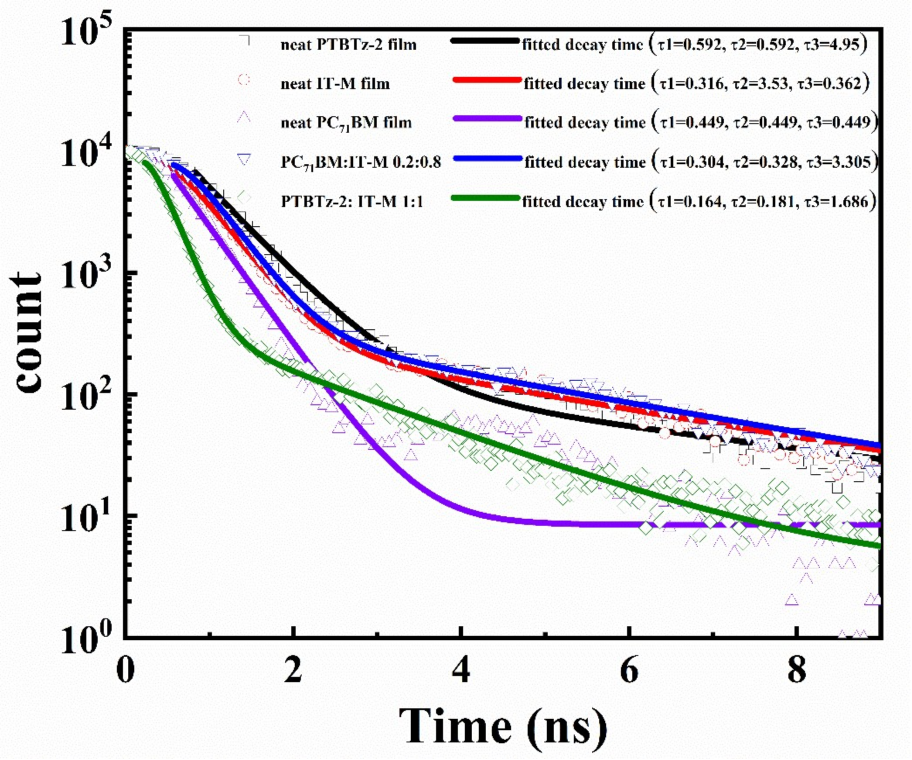

Figure S5. The TCSPC spectra of neat PTBTz-2 and neat IT-M films were measured by monitoring 720 nm and 750nm emission respectively, under the light excitation of 600 nm pulse NanoLED source. And the neat $PC_{71}BM$ film were excited at 433nm and probed at 708nm. The blend film of PTBTz-2: IT-M (1:1) were excited at 600nm and probed at 720nm and $PC_{71}BM$: IT-M (0.2:0.8) were excited at 433nm and probed at 708nm.

Table S4. The fitted lifetime of neat PTBTz-2, IT-M and $PC_{71}BM$ films and the blend films of PTBTz-2: IT-M (1:1) and $PC_{71}BM$: IT-M (0.2:0.8).

	A_1	τ_1(ns)	A_2	τ_2(ns)	A_3	τ_3(ns)
PTBTz-2	6177.37	0.592	2114.31	0.592	157.29	4.954
IT-M	-12526.22	0.316	310.48	3.537	17266.16	0.362
$PC_{71}BM$	955.59	0.449	3272.54	0.449	2129.87	0.449
$PC_{71}BM$: IT-M (0.2:0.8)	-9043.81	0.304	11607.51	0.328	340.14	3.305
PTBTz-2: IT-M (1:1)	-5094.75	0.164	7258.86	0.182	335.28	1.686

The lifetimes were fitted by Gaussian response function convoluted with a triple-exponential decay function (4) convoluted with a triple exponential decay function:

$$\Delta y(\mathrm{t}) = y_0 + A_1 \exp(\frac{-t}{\tau_1}) + A_2 \exp(\frac{-t}{\tau_2}) + A_3 \exp(\frac{-t}{\tau_3}) \qquad (4)$$

Transient Absorption and Pump-probe Measurements:

Femtosecond pump-probe spectroscopy was performed to measure transient absorption changes (optical density changes, ΔOD). A high energy laser pulse (pump) is sent onto the sample, then a second pulse with weak intensity probes the optical perturbation induced by the pump after a variable delay. The laser beam is supplied by amplified titanium: sapphire laser source (800 nm, Coherent) that provides 30 fs pulses with a repetition rate of 1 kHz. This beam having a power of 6 W is split into two parts. The most intense part (4 W) is used as the pump beam after passing through an optical parametric amplifier (Opera solo) which enables to tune its wavelength over a wide spectrum, while the other weak probe beam is converted into a white-light supercontinuum after focusing on a calcium fluoride crystal. The pump-probe delay control is ensured by a retroreflector mirror mounted on a high-precision mechanical translation stage and set on the probe path. Pump and probe field polarizations are linear and perpendicular to each other. And 3D transient spectral image ΔOD(λ,t) was formed when the delay line was scanning. The 1024-pixel imaging spectrometer (CDP2022i) can record the spectral and temporal profiles of the transient absorbance changes via serial port connection to the computer. Two photodiode arrays were placed after the imaging spectrometer to measure probe and reference pulses simultaneously, originating from femtosecond continuum (femtosecond white light). Photoinduced optical density (absorbance) changes were calculated as $\Delta \mathrm{OD}_\lambda = -\lg((I_\lambda^{probe}/I_\lambda^{ref})_{ex}/(I_\lambda^{probe}/I_\lambda^{ref}))$, where $(I_\lambda^{probe}/I_\lambda^{ref})_{ex}$ is a ratio for the corresponding pump and reference signals at given wavelength, measured after the sample excitation, and $(I_\lambda^{probe}/I_\lambda^{ref})$ is a corresponding ratio for the unexcited sample. The data were plotted as a function of delay time and wavelength by further processing at ExiPro 2.8.6 software.

The intensity of the pump laser fluence are 20 μJ cm^{-2} for 380nm excited and 400nm excited light.

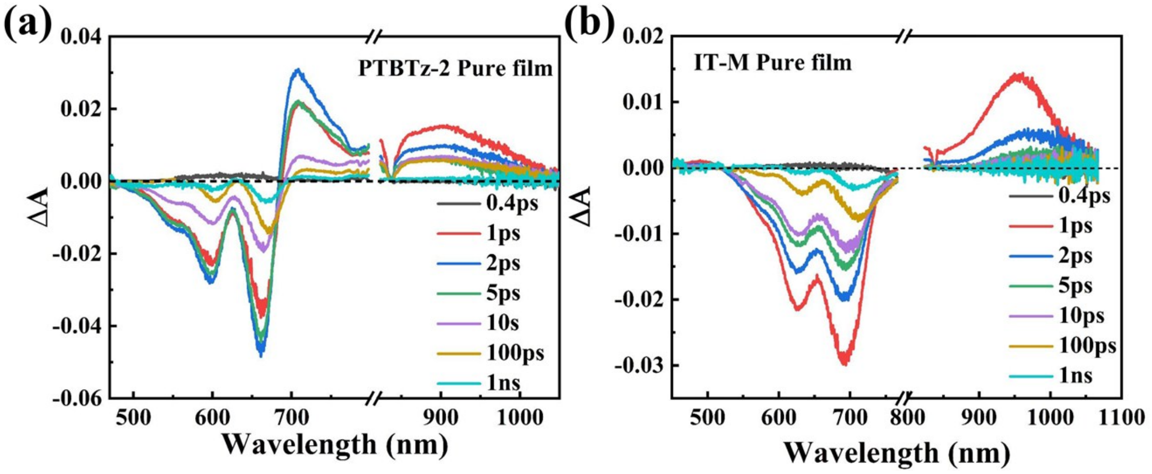

Figure S6. The femtosecond time-resolved transient absorption spectra of: (a) neat PTBTz-2 and (b) neat IT-M film.

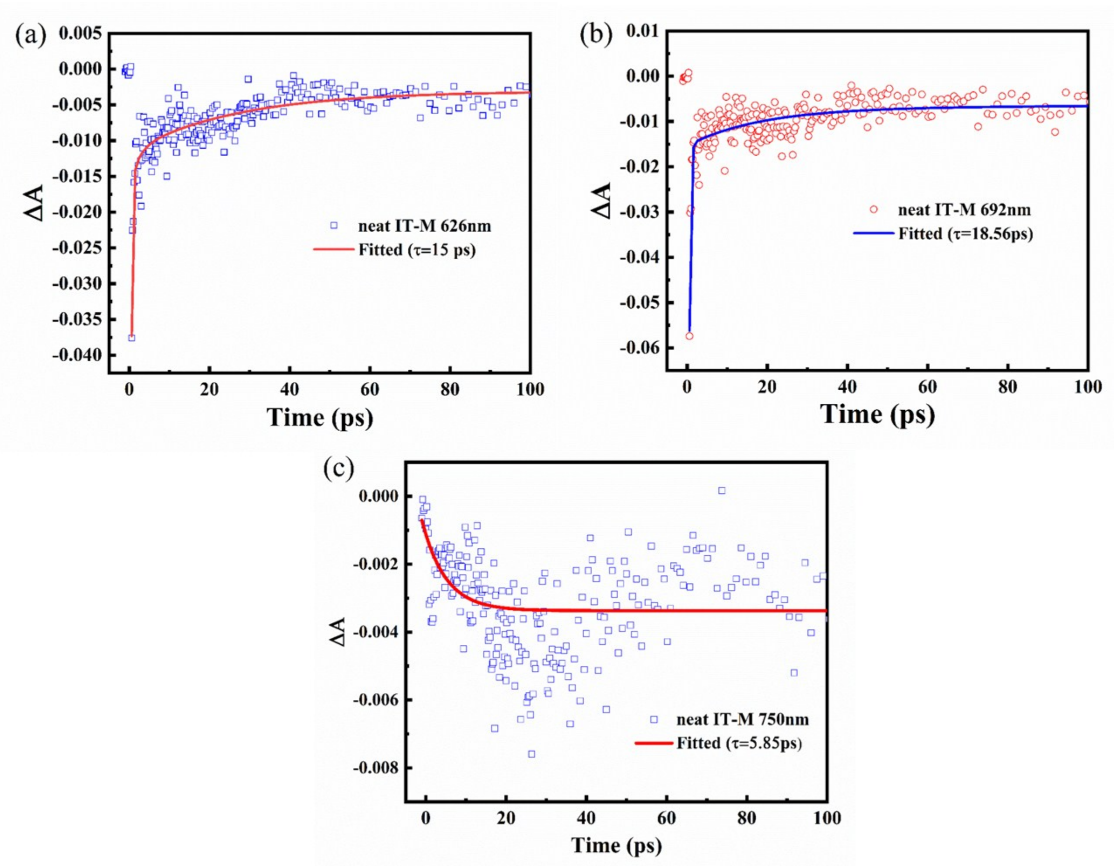

Fig. S7 (a), (b) and (c) are Dynamics of the neat IT-M film at 626nm, 692nm and 750nm, respectively.

References

1. J. Li, Y. Wang, Z. Liang, N. Wang, J. Tong, C. Yang, X. Bao and Y. Xia, *ACS Appl. Mater. Interfaces*, 2019, **11**, 7022-7029.

2. T. Liu and A. Troisi, *Adv. Mater.*, 2013, **25**, 1038-1041.

3. D. Li and A. W. Neumann, *Journal of Colloid and Interface Science*, 1990, **137**, 304–307.

4. M. Sumita, K. Sakata, S. Asai, K. Miyasaka and H.Nakagawa, *Polym. Bull.*, 1991, **25**, 265–271.